

Network Capacity Optimisation in Millimetre Wave Band Using Fractional Frequency Reuse

NASER AL-FALAHY^{1,2} AND OMAR Y. K. ALANI¹

¹University of Salford, Manchester M5 4WT, U.K.

²University of Anbar, Ramadi 31001, Iraq

Corresponding author: Naser Al-Falahy (n.f.a.al-falahy@edu.salford.ac.uk)

This work was supported by the Ministry of Higher Education and Scientific Research, University of Anbar, Iraq.

ABSTRACT Inter cell interference (ICI) is a major challenge that degrades the performance of mobile systems, particularly for cell-edge users. This problem arises significantly in the next-generation system, as the trend of deployment is with high densification, which yields an ultra-dense network (UDN). One of the challenges in UDN is the dramatic increase of ICI from surrounding cells. A common technique to minimize ICI is interference coordination techniques. In this context, the most efficient ICI coordination is fractional frequency reuse (FFR). This paper investigates the FFR in UDN millimeter wave network at 26-GHz band. The focus is on dense network with short inter site distance, and higher order sectorisation (HOS). The metrics used in frequency reuse is the signal to interference plus noise ratio rather than the distance, as the line of sight in millimeter wave can be easily blocked by obstacles even if they are in close proximity to the serving base station. This paper shows that FFR can improve the network performance in terms of per user cell-edge data throughput and average cell throughput, and maintain the peak data throughput at a certain threshold. Furthermore, HOS has a potential gain over default sectorised cells when the interference is carefully coordinated. The results show optimal values for bandwidth split per each scenario in FFR scheme to give the best tradeoff between inner and outer zone users performance.

INDEX TERMS 5G network, fractional frequency reuse, higher order sectorisation, millimetre wave band.

I. INTRODUCTION

THE fifth generation (5G) is the next generation of wireless system for mobile networks to achieve very low latency, higher spectral efficiency, high data throughput, and to provide flexibility in design and implementation [1].

Due to the popularity of data hungry devices such as smart phones and tablets, this has increased the demands for faster mobile data traffic. Mobile networks operators face the need to install dense high capacity base stations (BSs) as well as small cells. These base stations should cover not only wide range but also hot-spots with fast, flexible and dynamic supply to cope with the unpredictable future users requirements.

5G networks have more challenges in improving the overall spectral efficiency, and reducing the operational and deployment cost. And since the trend of next generation network is ultra-dense network (UDN), Inter-Cell Interference (ICI) will be a challenging issue in 5G network.

In a cellular communication system, ICI is one of the main factors that impact the data throughput at the cell-edge zone, which consequently reduce the spectral efficiency of the

base station. Mobile systems have two frequency assignment techniques. In the first one, base stations transmit different frequencies, where each sector uses 25 per cent of the bandwidth. Here the reuse factor is 25%, and called Frequency Reuse Factor 3 (FRF₃). This scheme can highly minimise the co-channel interference among nearby cells, however, it reduces the spectrum efficiency. This technique has been used in Global System for Mobile Communication (GSM). In 3G/4G networks, all cells have the same carrier frequency and same bandwidth (reuse factor is 100 per cent), and called Frequency Reuse Factor 1 (FRF₁), which increases the spectrum efficiency but at the expense of increasing the interference from nearby cells [2].

Another technique can trade-off the aforementioned frequency reuse techniques, where every cell can transmit in the same frequency in the centre area; allocating the major part of the resources to this area, while the cell-edge area will use different resources to reduce interference, this technique known as Fractional Frequency Reuse (FFR) [2], [3]. FFR divides the coverage area of the cell into inner and

outer zones, where different FRFs are implemented in these regions to minimise the interference and increase the average spectral efficiency.

In [4], FFR was proposed to balance the peak data throughput and the average and cell-edge data throughput in cell area. The authors in [3] and [5] have proposed FFR with uniform power distribution and introduced the principle of capacity density and bandwidth density in Long Term Evolution (LTE) network, where their results show a noticeable improvement in cell-edge performance. While in [6], FFR was introduced in order to combat inter cell interference (ICI) in LTE network, the authors have evaluated two FFR scenarios, namely, FFR and Soft Frequency Reuse (SFR). The authors have compared them with the frequency reuse scheme in LTE network. A distance dependant frequency reuse scheme has been proposed in [7] with irregular macro base station placements, the author have derived new equations for signal to interference plus noise ratio (SINR) and uses difference power profile for BS transmission to optimise the network capacity. Nonetheless, SFR has better spectral efficiency but higher interference compared with FFR. This is due to the fact that the spectrum dedicated for the cell edge may also be used in the central zone if it is not being used at the cell edge [8].

Frequency reuse in millimetre wave band (mm-wave) has first proposed by V. Roman in [9], particularly in the local multipoint distributed service (LMDS) band at 28GHz. The author has shown a frequency reuse range of 1 up to 8 per cell, in addition to use polarisation and sectorisation to boost system capacity in this band.

FFR optimisation in this paper is aimed at maximising the cell-edge area data throughput (edge TP) and average user data throughput (avg TP), while maintaining the peak throughput (peak TP) at a certain threshold. The focus is on using higher carrier frequency; particularly in 26GHz band, where there is a precious bandwidth (24.25-27.5)GHz available for ultra-dense very high capacity networks in the UK [10]. This band has a high dependency on line of sight (LOS) due to their weak signal as result of high path loss and atmospheric attenuation. FFR is also important especially in higher order sectorisation (HOS) scenario in millimetre wave band [11] due to the increased interference as we will see in this paper. In HOS, ICI is growing dramatically due to the increased nearby cell interference. And the usage of FRF_1 will result in severe ICI, particularly at the cell-edge area, which degrade the network performance in terms of coverage and capacity [12]. Therefore, interference coordination is necessary to handle the excess interference and improve the cell performance.

This FFR split scenario take the advantage of both FRF_1 and FRF_3 by splitting the cell area into two areas: inner and outer zones. The bandwidth B_T is also partitioned into an inner band B_{inn} and outer band B_{out} . The inner zone is reused by all user equipment's (UEs); with a reuse factor of 1 (FRF_1) and therefore has a Full Reuse (FR) spectrum. On the other hand, the outer zone utilises a higher reuse factor (FRF_3) to

help combat ICI at the cell-edge zone, and thus, it has Partial Reuse (PR) spectrum [5].

The simulation of millimetre wave band is motivated by the spread of ray tracing tools that can predict the path loss and channel model of millimetre wave band. And also support diffuse scattering prediction model that greatly improves simulation accuracy for millimetre wave systems being developed for 5G. Wireless InSite® [13] and ICS Telecom/Designer by ATDI [14] have the potential to support higher frequency band, and considered as a high-fidelity ray tracing solvers for radio network planning and optimisation.

The rest of the paper is structured as follow: the network model is illustrated in section II, with a brief discussion on millimetre wave band. Section III discusses the problem optimisation and presents its formulation. In section IV, the performance metrics is clarified, which is the data throughput. The resources assignment in FFR scheme is discussed in section V and our proposed algorithm is presented. After that, the simulation result and discussion is illustrated in section VI. The use of FFR in higher order sectorisation network is discussed in section VII. Finally, the conclusions are drawn in section VIII.

II. NETWORK MODEL

The network model is illustrated in fig.1, it consists of millimetre wave nodes that connect a number of User Equipment (UEs) that either lie in inner zone supporting FRF_1 or outer zone which support FRF_3 . The UE SINR will decide whether this UE fall in either region. In this context, SINR threshold is defined so that any UE will exceed this threshold will be considered in the inner zone with FRF_1 , while UEs fail to achieve this threshold will be in the area of FRF_3 (cell-edge area), in this area, FRF_3 aim to improve the SINR on the account of reduced resources.

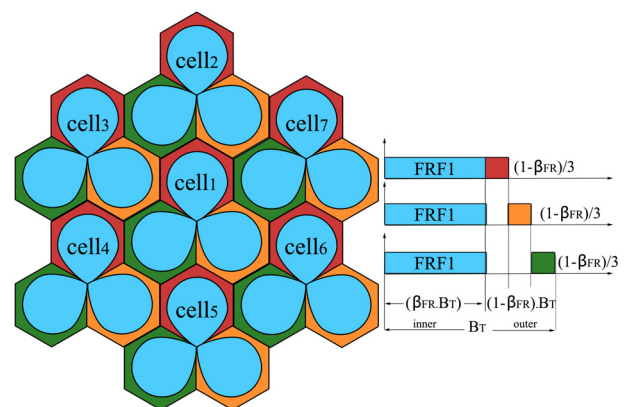


FIGURE 1. Network model showing the FFR frequency assignment, the sky-blue is the part of the bandwidth assigned to the inner zone with (FRF_1), while the coloured parts are for partial assignment with (FRF_3).

Most FFR/SFR schemes depend on the distance between BS and UE to judge whether UE lies in inner zone or in outer zone. The distance calculation is a complex issue that could

dramatically increase the complexity of FFR/SFR algorithm. It also ignore nearby UEs that has low SINR due to bad channel condition.

In millimetre wave band, however, UEs can be in a bad channel condition (low SINR) when the LOS is blocked by obstacles, even if they are in close proximity to their serving base stations. In order to take into account nearby UEs with low SINR, the split between inner/outer zones in this work is decided by UEs SINR. A threshold of SINR is set in the proposed algorithm for resource assignment, which split the region into two parts. UEs with low SINR will be treated as a cell-edge (outer zone), in which the algorithm will assign these UEs a sub-band that do not interfere with inner zone. While UEs having high SINR figures will be considered as inner zone, with full frequency reuse. These two zones will have two different schedulers that are used to simultaneously schedule the UEs of these regions. Details of simulation parameters are listed in table 1.

TABLE 1. Network model parameters.

Model parameter	Value
Multiple access	OFDMA
Network size	21 cells /10UEs per cell, with 25 surrounding interfering cells
Tx Power	40 dBm
Tx antenna gain G_{Tx}	18 dB
Rx antenna gain G_{Rx}	0 dB
Tx pattern	As in eq.1
Electrical tilt	- 6 degree (down tilt)
Rx pattern	Omni-directional
Carrier frequency	26GHz
Bandwidth	500MHz
Speed of light	299792458 m/s
Tx Antenna height	10 m
Rx antenna height	1.5 m
Inter site distance	150m
Modulation	Adaptive (QPSK, 16QAM, 64QAM)
Region of interest	ROI = 600x600 m
Noise Figure	10 dB
Traffic Model	Full Buffer
Scheduling	Round Robin & Proportional fair

Orthogonal Frequency Division Multiple Access (OFDMA) has been used as the multiple access in this model due to its powerful performance in dealing with multipath signals and compatibility with multi input multi output (MIMO) antennas. In OFDMA, the bandwidth is divided into small divisions called physical resource blocks (PRB) where each PRB is 180 kHz and has 12 adjacent OFDM subcarriers [15]. The single PRB is allocated to a single device for at least single transmission time interval (TTI) that is equal to 1ms. In our analysis, a uniform power distribution is implemented for all transmitting base stations for both inner zone and outer zone (cell-edge), with a worst case that all these BSs are transmitting at full power. Therefore, with uniform power profile and SINR threshold γ_{th} , a user located at (x,y) point in the cell area will be either in inner or outer zones

according to:

$$UE_i \in \begin{cases} \gamma_{i,UE(x,y)} \leq \gamma_{th}, UE(x,y) \in FRF_3 \\ \gamma_{i,UE(x,y)} > \gamma_{th}, UE(x,y) \in FRF_1 \end{cases} \quad (1)$$

A. MILLIMETRE WAVE BAND

When higher network capacity and connectivity is required, additional amount of spectrum is required as a result. And mobile network operators have improved the network capacity through utilizing additional bandwidth (higher frequency and wider bandwidth). Therefore, it is expected that 5G network will utilise higher bandwidth, such as utilising mm-wave band due to the very wide available bandwidth [16].

The Federal Communications Commission (FCC) has released many bands within mm-wave band to be used as a promising candidate for future 5G mobile system, including the local multipoint distribution service (LMDS) band from 28 to 30 GHz, 14GHz at the license-free band at 60 GHz, as well as 12.9 GHz located at 71–76 GHz, 81–86 GHz, and 92–95 GHz from the E-band [17], [18]. The office of communication in the UK (Ofcom) has released the 26GHz band in the UK [10]. And due to their small wavelengths, millimetre wave suffer high path loss (as per eq.2) and high atmospheric attenuation as shown in fig.2, thus has limited coverage [28].

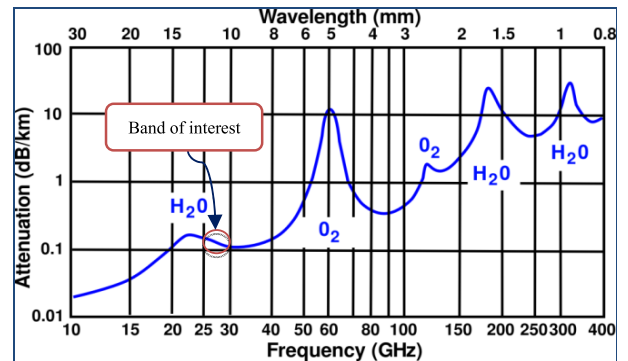


FIGURE 2. Average atmospheric attenuation of mm-wave [19].

The transmitting nodes have three sectors with directional antennas, the patterns is:

$$A(\theta) = -\min \left[12 \left(\frac{\theta}{\theta_{3dB}} \right)^2, A_m \right] \quad \text{where } -180 \leq \theta \leq 180 \quad (2)$$

where θ_{3dB} is the 3dB beamwidth that corresponds to 65 degrees, and $A_m = 20$ dB represents the maximum attenuation.

B. PATH LOSS

The path loss between a base station and connected UE is defined by the channel model [20]:

$$G_{ch} = 32.4 + 20 \log_{10}f + 10 a \log_{10}R + X_{\sigma} \quad (3)$$

where: G_{ch} is the channel gain between BS and UE in dB, f is the carrier frequency in GHz, R is the separation between base station and device in metres, α is the path loss exponent, and X_σ is the shadow fading loss which can be represented by log normal shadowing, that has zero mean and 9dB [21], [22] standard deviation. Fig.3 shows the path loss and SNR mapping for path loss map (left) and path loss and shadow fading map (right).

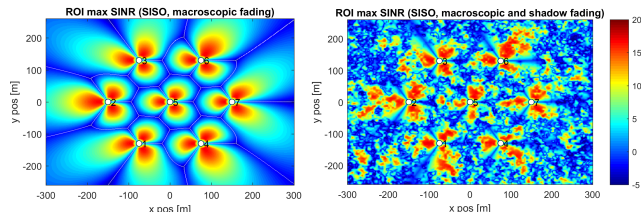


FIGURE 3. SINR mapping of mm-wave sites, left is the path loss map, and right is the path loss plus shadow fading map.

Due to the high path loss and atmospheric attenuation, millimetre wave has higher dependency on LOS in its propagation model, as reflected signals (multipath) are weak in general. Therefore, the antenna type used in this work is a single input single output (SISO), due to the fact that multiple input multiple output (MIMO) antennas relies on multipath to achieve the spatial multiplexing gain. However, an alternative approach for MIMO in LOS is the millimetre-wave MIMO, which establishes multiple parallel links in a LOS environment through spatially distributed antennas [23], [24]. The basic theory for LOS MIMO architecture first appeared in [25].

III. THE PROBLEM OPTIMISATION

The adaptive resource assignment partitions the cell coverage area into two parts: cell centre with full reuse and cell edge with partial reuse. The scheduler of FFR divides the total bandwidth B_T between these areas. Therefore, in three sectorised site, the total bandwidth of a sector is given by:

$$B_T = B_{inn} + B_{out} \tag{4}$$

where B_{inn} is the bandwidth of inner zone and B_{out} is the bandwidth of outer zone (cell-edge).

To manage the bandwidth partitioning more efficiently, β_{FR} is defined as the normalized FR bandwidth:

$$\beta_{FR} = \frac{B_{inn}}{B_T}, \text{ where } 0 \leq \beta_{FR} \leq 1 \tag{5}$$

Therefore, for a single cell (one sector), the total available bandwidth will be:

$$B_{FFR} = \beta_{FR} \cdot B_T + \frac{1}{3}(1 - \beta_{FR})B_T \tag{6}$$

where: B_{FFR} is the bandwidth for single cell in FFR network.

Given that $B_{FFR} \leq B_T$:

For $\beta_{FR} = 0$,

$$B_{FFR} = \frac{B_T}{3}, \text{ Similar to } FRF_3 \tag{7}$$

and for $\beta_{FR} = 1$,

$$B_{FFR} = B_T, \text{ Similar to } FRF_1 \tag{8}$$

This means that there will be a reduction in the amount of total usable bandwidth. And users in inner zone do not share the bandwidth with outer zone, which minimise the interference for centre UEs and cell-edge UEs. Table 2 shows the bandwidth split for different values of β_{FR} from a total bandwidth of 500MHz.

TABLE 2. Available bandwidth for FR/PR zones according to β_{FR} setting.

β_{FR}	B_{inn} MHz	B_{out} MHz
1	500	
0.9	450	50/3
0.8	400	100/3
0.7	350	150/3
0.6	300	200/3
0.5	250	250/3
0.4	200	300/3
0.3	150	350/3
0.2	100	400/3
0.1	50	450/3
0	500/3	

The purpose here is to find the best trade-off for β_{FR} to maximize the average cell throughput ($A_v TP$) and the cell-edge throughput (Edge TP), while maintaining the peak data throughput at certain threshold. Therefore, the optimisation problem can be written as:

$$\begin{aligned} & \max. (A_v TP, Edge TP) \\ & \beta_{FR} \in [0, 1] \\ & peak TP \leq r_T \end{aligned} \tag{9}$$

where r_T is the minimum required peak data throughput.

IV. DATA THROUGHPUT

The data throughput of cellular network has an upper theoretical bound represented by the well-known Shannon formula [26]:

$$R_b \leq c = B \log_2 (1 + \gamma_i) \tag{10}$$

where:

$$\gamma_i = \frac{S}{I + N} \tag{11}$$

γ_i is the SINR, B is the allocated bandwidth, S is the signal power of the serving cell, I represents the interference from all surrounding cells, and N denotes the thermal noise power.

And due to the frequency reuse scheme which split the UE according to their SINR and split the entire bandwidth into two parts, therefore, we will have two data throughput per cell. R_{FRF1} for centre zone implementing FRF_1 and R_{FRF3} for outer zone (cell-edge) implementing FRF_3 . And the total

cell throughput is the sum of throughput in inner and outer zone:

$$R_{tot} = \begin{cases} R_{FRF_1} (\gamma_i > \gamma_{th}), UE_i \in FRF_1 \text{ zone} \\ R_{FRF_3} (\gamma_i \leq \gamma_{th}), UE_i \in FRF_3 \text{ zone} \end{cases} \quad (12)$$

where,

$$R_{FRF_1} = \beta_{FR} * B_T \log_2(1 + \gamma_i(\gamma_i > \gamma_{th})) \quad (13)$$

$$R_{FRF_3} = \frac{(1 - \beta_{FR})}{3} B_T \log_2(1 + \gamma_i(\gamma_i \leq \gamma_{th})) \quad (14)$$

Therefore, the average cell throughput is:

$$R \leq c = \sum_{UE_{\gamma_i=-\infty}}^{\gamma_{th}} R_{FRF_3} + \sum_{UE_{\gamma_i=\gamma_{th}}}^{\infty} R_{FRF_1} \quad (15)$$

V. RESOURCES ASSIGNMENT

The simulation and resource assignment of FFR scheme in cellular network is represented by the pseudo code in algorithm1. The simulation is initialised by defining the Region of Interest (ROI), in which all BSs and UEs are generated inside. The simulation length will last for 50 TTIs. The physical resource blocks PRB is defined according to the allowed bandwidth. And in this stage, two important parameters are defined in this step, namely: SINR threshold (γ_{th}) and the normalized bandwidth (β_{FR}). Furthermore, due to the split of bandwidth (resources), two schedulers can be called to schedule the resources of inner zone and outer zone, simultaneously. In this work, round robin (RR) and proportional fair (PF) scheduling algorithms have been used as the scheduler for FR/PF zones. There are no restrictions on using any other scheduling algorithms, and different schedulers can be used for FR/PR zones, simultaneously. The simulation will check the available devices that request resources and check their SINR, compare it with γ_{th} , in order to split the FR zone from PR zone. If a UE SINR is equal to, or less than γ_{th} , then this UE will be assigned to PR zone where a certain scheduler will be responsible for the resource scheduling, with a total bandwidth of $(1 - \beta_{FR}).B_T/3$. Otherwise, if the UE SINR is larger than γ_{th} , this UE will be assigned to the FR zone with a different scheduler that is responsible on resources assignment of similar UEs, with a bandwidth of $\beta_{FR}.B_T$. Both schedulers will assign their resources until all available PRB is exhausted. When the allowed TTI is reached, the simulation will be concluded and the data throughput for both regions is aggregated.

VI. SIMULATION RESULTS AND DISCUSSION

For worst case consideration in terms of inter cell interference, all cells are transmitting at full power. The SINR calculation (see fig. 4) of the UEs in simulation is determined by calculating the received power of each UE according to Friis formula [27]:

$$p_r = p_T + G_T + G_r - L_p \quad (16)$$

Where: p_r is the received power, p_T is the transmitted power by the cell (radiation pattern) according to eq.(2), G_T , G_r are

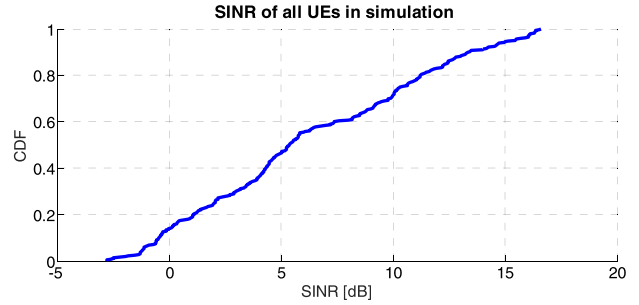


FIGURE 4. CDF of all UEs SINR in simulation.

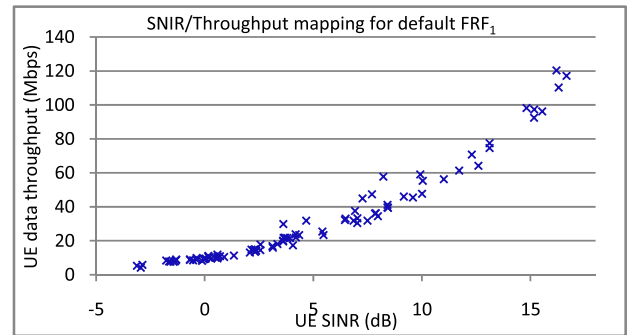


FIGURE 5. SINR to throughput mapping of FRF₁ scheme network.

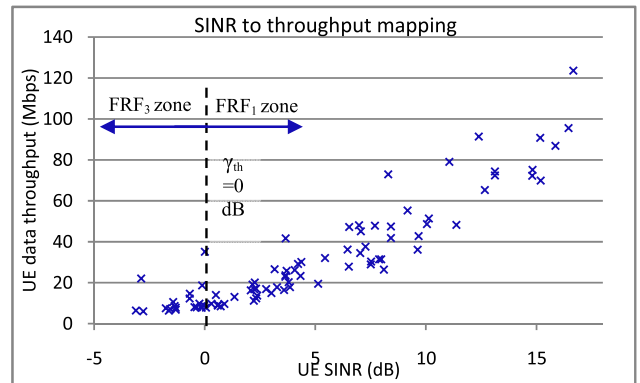


FIGURE 6. SINR to throughput mapping of FFR scheme network, with $\gamma_{th} = 0\text{dB}$, and $\beta_{FR} = 0.7$.

the gain of transmitting and receiving antennas, respectively. In this work, $G_T = 18$ dBi, while $G_r = 0$. L_p denotes the signal path loss according to eq.(3).

The transmitting BS are at 10m in height [20], [28], [29], while UEs are at a height of 1.5m, with inter site distance of 150m.

The SINR to throughput mapping in fig. 5 shows the UEs data throughput with respect to UE SINR with normal frequency reuse, FRF₁, where only one zone available, implementing round robin scheduling. In this scheme, the peak throughput is 57Mbps, edge throughput = 6.27Mbps, with average cell throughput = 188.53 Mbps. On the other hand, fig.6 depicts the SINR to throughput mapping of FFR scheme network, with $\gamma_{th} = 0\text{dB}$ and $\beta_{FR} = 0.7$. In this scenario, the

cell coverage has split into inner and outer zone, with FFR₁ and FFR₃, respectively. In this scenario, the cell-edge data throughput has improved to 9.26 Mbps (gain = % 47.47), and the average cell throughput has improved to 226.69 (gain = %20.23). While the peak data throughput is 66.28Mbps with %16.27 gain over full reuse frequency scheme FRF₁. Lower values of β_{FR} can further improve cell-edge data throughput, but on the expense of loss in peak data throughput.

Therefore, aggregating the data throughput of both zones has yield fig.7, which demonstrates the potential gain in average and cell-edge per user data throughput in the case of interference coordination, on the account of lower peak data throughput. This figure shows the relation between the peak/average data throughput and cell-edge data throughput as a function of the normalized bandwidth β_{FR} .

Algorithm 1 Pseudo Code of Resource Assignment

- 1: **Define** ROI % region of interest
- 2: **Set** TTI=1ms
- 3: Define two scheduler, Round Robin & Proportional fair
- 3: Set Simulation time=50 TTI
- 4: Generate cells per ROI
- 5: Set finite UEs per cell
Set SINR threshold to γ_{th}
Set β_{FR} as per user setting
- 6: **for** each TTI **do**
- 7: Check available UEs SINR/available resources N_{PRB}
- 11: **for** each Tx Node **do**
- 12: Check whether UE SINR below or above γ_{th}
- 13: **if** $UE_i \text{ SINR} > \gamma_{th}$, **then**
Set $b.w = (\beta_{FR}) * B_T$
Pick a scheduler (RR/PF)
Schedule these UEs according to FRF₁
- 14: **else, if** $UE_j \text{ SINR} \leq \gamma_{th}$, **then**
- 15: Set $b.w = ((1 - \beta_{FR})/3) * B_T$ %three sector cell
Pick a scheduler (RR/PF)
- 16: Schedule these UEs according to FRF₃
- 18: **end if**
- 19: Aggregate cell throughput for both zones
- 20: Calculate average/peak/edge data throughput
- 21: **end for**
- 22: **end for**

An optimum value for β_{FR} can be chosen according to this figure, so that an improvement in cell-edge data throughput is achieved while keeping the peak throughput at a certain threshold. This will consequently improve the overall all cell data throughput. This figure is the result of using round robin scheduler for both FR/PR zones.

Fig.8 depicts the same scenario but with proportional fair scheduling been used for both FR/PR zones. An improvement in term of data throughput is noticeable here, however, doesn't change the optimum β_{FR} allocation. For both figures, a β_{FR} of 0.7 can give improvement for cell-edge user while

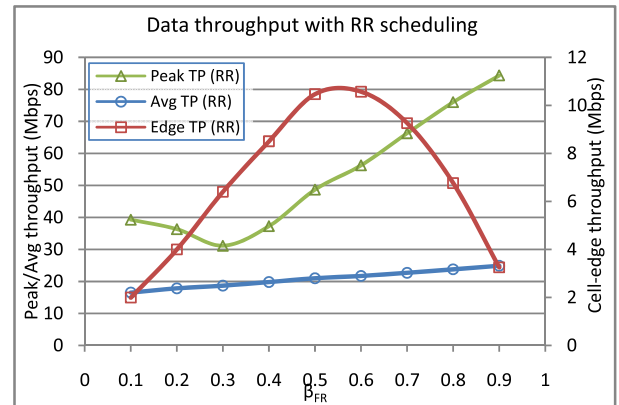


FIGURE 7. Average/cell-edge data throughput in three sector site with RR scheduling.

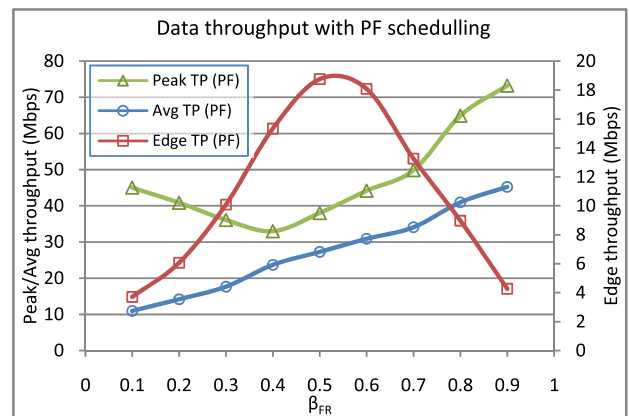


FIGURE 8. Average/cell-edge data throughput in three sector site with PF scheduling.

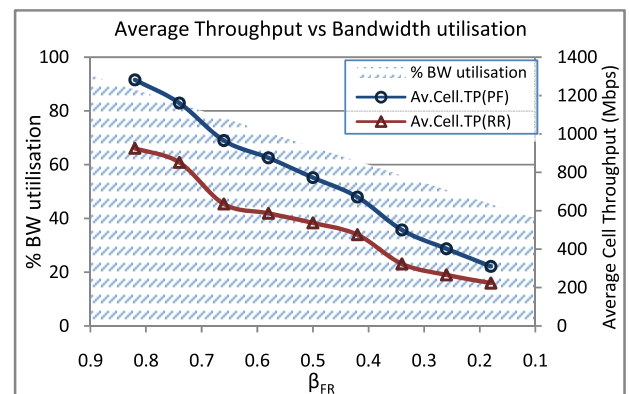


FIGURE 9. Bandwidth utilisation with average cell throughput as a function of β_{FR} .

keep the peak data throughput loss at a minimum level. Fig. 9 shows the average cell throughput of both schedulers along with the bandwidth utilisation as a function of β_{FR} . Lower values of β_{FR} can further improve cell-edge user performance, however, it can dramatically decrease the bandwidth utilisation, and hence, the overall cell performance.

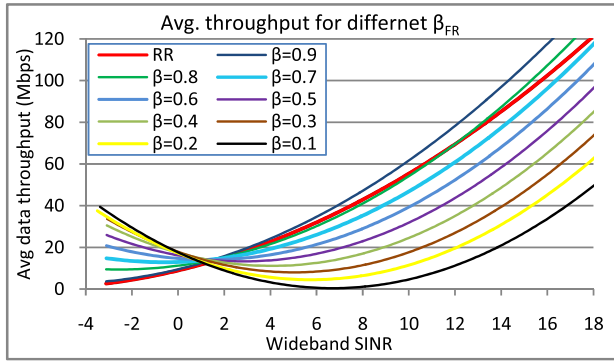


FIGURE 10. Balance between inner and outer zone with respect to β_{FR} .

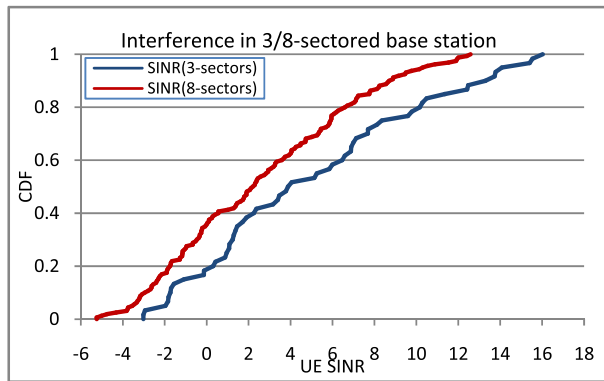


FIGURE 11. Interference in HOS in terms of SINR.

While in fig. 10, the relation between balancing cell-edge and average UE throughput has been illustrated as a function of β_{FR} . It demonstrates how the value of β_{FR} can balance the capacity between split zones, where a ranges of β_{FR} values from RR: round robin scheduling implementing FRF_1 as $\beta_{FR} = 1$ to a minimum of $\beta_{FR} = 0.1$, a β_{FR} in the range of 0.7 to 0.8 can give the best trade-off between the performance of inner and outer zones. Low value of β_{FR} , e.g. 0.1 can result in significant improvement in cell edge zone data throughput; however, it will dramatically decrease the inner zone data throughput. On the other hand, high figure of β_{FR} , e.g. 0.9 can result in high throughput in inner zone, on the account of low throughput in outer zone UEs.

VII. FREQUENCY REUSE IN HIGHER ORDER SECTORISATION

As millimetre wave has high directionality and dependency on line of sight, it is anticipated that higher order sectorisation (HOS) is used to further increase the network capacity and boost its performance. In [30], the authors have proposed a six sectored order for the base station, in order to improve the system throughput through the spatial multiplexing and interference coordination. However, higher inference is expected due to the new surrounding sectors transmitting at the same carrier frequency [11] as shown in fig.11, where interference is compared between three and eight sectored

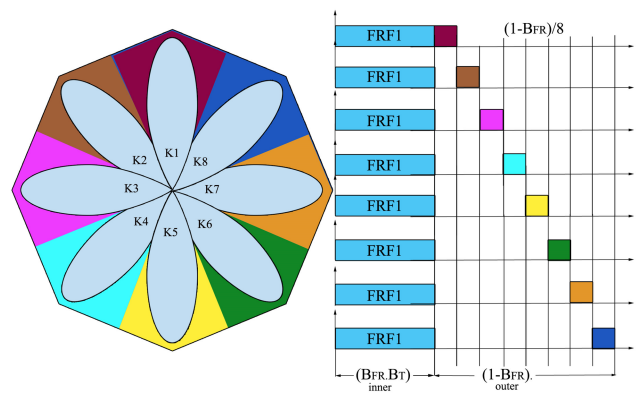


FIGURE 12. Network model showing the FFR frequency assignment for HOS.

cell, in terms of UE SINR. It has been seen that around 5dB loss in UE SINR in eight sector scenario compared with the default three sectored sites. It's worth mentioning that some contributions claim that an order of eight achieves no gain over six sectorisation due to the excess interference, and therefore, suggested that sectorisation is kept up to six.

In such scenario, FFR scheme has been applied to eight sectored cell, which will split the coverage area into two regions: inner and outer zone. However, the bandwidth will be split into FR band for inner zone plus eight PR sub-bands for outer zone, where:

$$B_{inn} = \beta_{FR} \cdot B_T, B_{out} = \frac{1}{8} (1 - \beta_{FR}) \cdot B_T \quad (17)$$

Fig.12 depicts the 8-sectored base station with FFR scheme. Every colour denotes a sub band that is assigned to the cell-edge users of a single sector. Therefore, the total bandwidth for a single sector can be written as:

$$B_{FFR} = B_{inn} + B_{out} = \beta_{FR} \cdot B_T + \frac{1}{8} (1 - \beta_{FR}) B_T \quad (18)$$

And therefore, the data throughput for each zone will be: for inner zone:

$$R_{FRF_1} = \beta_{FR} * B_T \log_2 (1 + \gamma_{i(\gamma_i > \gamma_{th})}) \quad (19)$$

and for outer zone:

$$R_{FRF_3} = \frac{(1 - \beta_{FR})}{8} B_T \log_2 (1 + \gamma_{i(\gamma_i \leq \gamma_{th})}) \quad (20)$$

In HOS, new sectors have been added to take advantage of the directionality of millimetre wave. However, the new sectors have generated a new interference, as recently showed in fig.11. This makes some UEs which lie between these sectors to have low SINR, making them to be assigned to the outer zone consideration, with partial frequency reuse. Fig.13 demonstrates this case, where the SINR mapping is shown for eight sectored base station. Dots denote UEs assigned in the inner zone with full frequency reuse, whereas crosses denote UEs assigned in the cell-edge zone with partial frequency assignment.

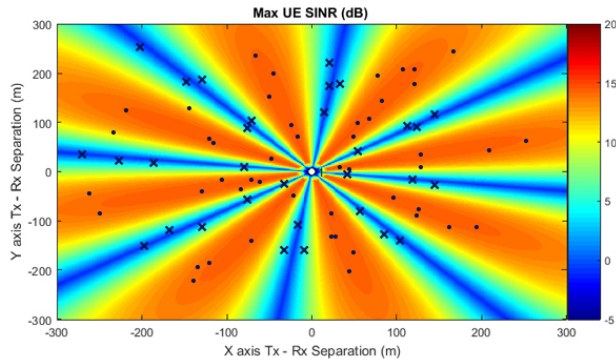


FIGURE 13. Eight sectored base station, with FFR scheme; dots represent the UEs with full reuse (FRF₁), while the crosses represent UEs with partial reuse (FRF₃).

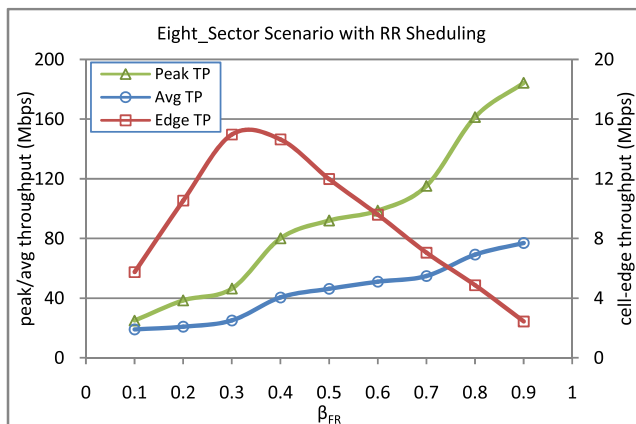


FIGURE 14. Average/cell-edge data throughput in HOS with RR scheduling.

Likewise the default three sectored BS, the average cell throughput is decreasing as the value of β_{FR} is decreased. And the cell-edge users will benefit from decreasing β_{FR} . Therefore, an optimal value of β_{FR} can be derived so that to achieve the optimised solution, where the cell-edge throughput is improved on the account keeping the peak throughput at a certain threshold. The average cell throughput is improved as a result.

Fig. 14 depicts this case, where the peak/average/cell-edge data throughput in Mbps - with round robin scheduling - is shown with respect to different values of β_{FR} . As per this figure, a value of $\beta_{FR} = 0.6$ is seen to provide the best trade-off to improve the outer zone data throughput while keep the inner zone user at a certain threshold. Fig. 15 shows the same case with proportional fair schedulers. It's noticed that the optimal value of β_{FR} has been shifted by a 0.1 in HOS scheme, which equal to %10 of the total bandwidth, compared with default three sectored base station. This shift is justified by the higher number of sectors and the increased ICI, which make the cell-edge zone demands more bandwidth to cope with ICI and improve their UEs data throughput.

Generally, there are gains as a result of using FFR scheme as well as HOS in millimetre wave band. Therefore, in order

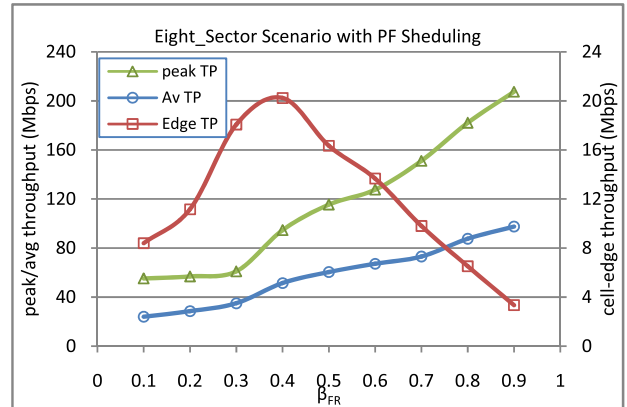


FIGURE 15. Average/cell-edge data throughput in HOS with PF scheduling.

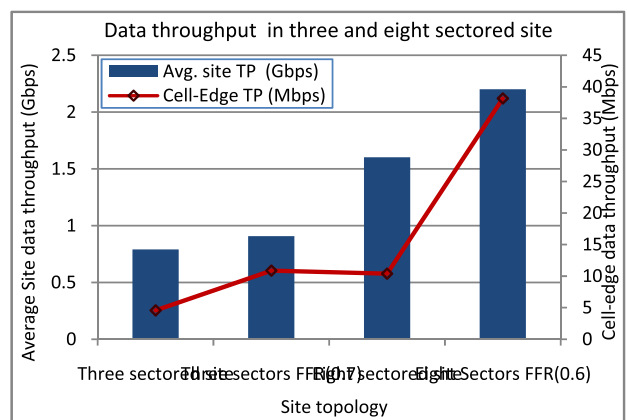


FIGURE 16. FFR gain in three and eight sectored site.

to measure the gain, a simulation has been conducted assuming 40 UEs uniformly distributed around the transmitting site. In the first scenario, all sites are considered three sectored sites, without FFR. Then, FFR is implemented to see the gain. The same scenarios have been repeated with eight sectored site. As per fig.16, the gain per three and eight sectored site is shown in terms of both average site throughput (Gbps) and cell-edge data throughput (Mbps). Interference coordination has increased the overall network performance. And in the case of higher order sectorisation, FFR has reduced the interference, which led into a high gain compared with other sectored sites.

VIII. CONCLUSION

Due to the ultra-dense deployment represented by 5G deployment scenario, ICI will represent a serious challenge in future millimetre wave 5G systems. In this work, FFR interference coordination has been used to suppress interference in dense network at higher carrier frequency, particularly at 26GHz band.

Frequency reuse scheme is important in millimetre wave band to further boost the network capacity and improve its performance. In this context, FFR has been harnessed as interference coordination technique in order to combat ICI as

a result of the dense network. The new scheme has shown a significant improvement in network performance in terms of cell-edge user data throughput and average cell data throughput while maintain the peak throughput at certain threshold. Optimum values for the normalised bandwidth β_{FR} has been derived, for both three and eight sectored site, which give the best trade-off between cell-edge and center user performance. And with the right optimisation, eight sectored base stations can give the potential gain over three and six sectored base stations, to boost the network capacity.

REFERENCES

- [1] N. Al-Falahy and O. Y. Alani, "Technologies for 5G Networks: Challenges and opportunities," *IT Prof.*, vol. 19, no. 1, pp. 12–20, Jan./Feb. 2017.
- [2] C. Cox, *An Introduction to LTE, LTE-Advanced, SAE And 4G Mobile Communications*, 1st ed. Hoboken, NJ, USA: Wiley, 2012.
- [3] J. C. Ikuno, M. Taranetz, and M. Rupp, "A fairness-based performance evaluation of fractional frequency reuse in LTE," in *Proc. 17th Int. ITG Workshop Smart Antennas (WSA)*, Stuttgart, Germany, Mar. 2013, pp. 1–6.
- [4] M. Asaad, "Optimal fractional frequency reuse (FFR) in multicellular OFDMA system," in *Proc. IEEE 68th Veh. Technol. Conf. (VTC-Fall)*, Calgary, BC, Canada, Sep. 2008, pp. 1–5.
- [5] M. Taranetz, J. C. Ikuno, and M. Rupp, "Capacity density optimization by fractional frequency partitioning," in *Proc. 45th Asilomar Conf. Signals, Syst. Comput.*, Pacific Grove, CA, USA, Nov. 2011, pp. 1398–1402.
- [6] H. E. Elmutasim, O. M. Elfadil, M. A. I. Adil, and M. Abas, "Fractional frequency reuse in LTE networks," in *Proc. 2nd World Symp. Web Appl. Netw. (WSWAN)*, Sousse, Tunisia, Mar. 2015, pp. 1–6.
- [7] A. Adejo, S. Boussakta, and J. Neasham, "Interference modelling for soft frequency reuse in irregular heterogeneous cellular networks," presented at the 9th Int. Conf. Ubiquitous Future Netw. (ICUFN), Milan, Italy, Jul. 2017, pp. 381–386.
- [8] Y. S. Cho, J. Kim, W. Y. Yang, and C. G. Kang, *MIMO-OFDM Wireless Communications With MATLAB*. Hoboken, NJ, USA: Wiley, 2010.
- [9] V. I. Roman, "Frequency reuse and system deployment in local multipoint distribution service," *IEEE Pers. Commun.*, vol. 6, no. 6, pp. 20–27, Dec. 1999.
- [10] *Update on 5G Spectrum in the UK*, Ofcom, London, U.K., Feb. 2017, pp. 1–19.
- [11] N. Al-Falahy and O. Y. K. Alani, "The impact of higher order sectorisation on the performance of millimetre wave 5G network," in *Proc. 10th Int. Conf. Next Generat. Mobile Appl., Secur. Technol. (NGMAST)*, Cardiff, U.K., Aug. 2016, pp. 1–5.
- [12] A. S. Mohamed, M. Abd-Elnaby, and S. A. El-Dolil, "Self-organised dynamic resource allocation scheme using enhanced fractional frequency reuse in long term evolution-advanced relay-based networks," *IET Commun.*, vol. 10, no. 10, pp. 1163–1174, 2016.
- [13] Remcom. 2014. *Wireless InSite*. Accessed: Jan. 15, 2016. [Online]. Available: <https://www.remcom.com/wireless-insite>
- [14] ATDI. (2018). *ICS Designer The Most Complete and Cost-Effective Radio Planning and Optimization Tool*. Accessed: Jan. 29, 2018. [Online]. Available: <http://www.atdi.com/ics-designer/>
- [15] *LTE; Evolved Universal Terrestrial Radio Access (E-UTRA); Radio Frequency (RF) system scenarios (3GPP TR 36.942 version 10.3.0 Release 10)*, document TR 36.942, 3GPP, 2011.
- [16] "5G: What is it?" Ericsson, Stockholm, Sweden, White Paper, Oct. 2014, pp. 1–10. [Online]. Available: <https://www.ericsson.com/assets/local/news/2014/10/5g-what-is-it.pdf>
- [17] F. Boccardi, R. W. Heath, Jr., A. Lozano, T. L. Marzetta, and P. Popovski, "Five disruptive technology directions for 5G," *IEEE Commun. Mag.*, vol. 52, no. 2, pp. 74–80, Feb. 2014.
- [18] F. Khan and Z. Pi, "An introduction to millimeter-wave mobile broadband systems," *IEEE Commun. Mag.*, vol. 59, no. 6, pp. 101–107, Jun. 2011.
- [19] M. Marcus and B. Pattan, "Millimeter wave propagation: Spectrum management implications," *IEEE Microw. Mag.*, vol. 6, no. 2, pp. 54–62, Jun. 2005.
- [20] A. Ghosh *et al.*, "Millimeter-wave enhanced local area systems: A high-data-rate approach for future wireless networks," *IEEE J. Sel. Areas Commun.*, vol. 32, no. 6, pp. 1152–1163, Jun. 2014.
- [21] G. R. MacCartney, Jr., J. Zhang, S. Nie, and T. S. Rappaport, "Path loss models for 5G millimeter wave propagation channels in urban microcells," in *Proc. IEEE Global Commun. Conf.*, Dec. 2013, pp. 3948–3953.
- [22] T. A. Thomas and F. W. Vook, "System level modeling and performance of an outdoor mmWave local area access system," in *Proc. IEEE 25th Int. Symp. Pers., Indoor Mobile Radio Commun. Syst.*, Washington, DC, USA, Sep. 2014, pp. 108–112.
- [23] C. Sheldon, E. Torkildson, M. Seo, C. P. Yue, M. Rodwell, and U. Madhow, "Spatial multiplexing over a line-of-sight millimeter-wave MIMO link: A two-channel hardware demonstration at 1.2 Gbps over 41 m range," in *Proc. 1st Eur. Conf. Wireless Technol.*, Amsterdam, The Netherlands, Oct. 2008, pp. 198–201.
- [24] N. Al-falahy and O. Y. K. Alani, "The impact of base station antennas configuration on the performance of millimetre wave 5G networks," presented at the 9th Int. Conf. Ubiquitous Future Netw. (ICUFN), Milan, Italy, Jul. 2017, pp. 636–641.
- [25] D. Gesbert, H. Bolcskei, D. A. Gore, and A. J. Paulraj, "Outdoor MIMO wireless channels: Models and performance prediction," *IEEE Trans. Commun.*, vol. 50, no. 12, pp. 1926–1934, Dec. 2002.
- [26] N. Bhusan *et al.*, "Network densification: The dominant theme for wireless evolution into 5G," *IEEE Commun. Mag.*, vol. 52, no. 2, pp. 82–89, Feb. 2014.
- [27] A. Sayeed, J. Brady, P. Cheng, and U. Tayyab, "Indoor channel measurements using a 28 GHz multi-beam MIMO prototype," in *Proc. IEEE Veh. Technol. Conf.*, Montreal, QC, Canada, Sep. 2017, pp. 1–5.
- [28] N. Al-falahy and O. Y. K. Alani, "Design considerations of ultra dense 5G network in millimetre wave band," presented at the 9th Int. Conf. Ubiquitous Future Netw., Milan, Italy, Jul. 2017, pp. 141–146.
- [29] Z. Zhang, J. Ryu, S. Subramanian, and A. Sampath, "Coverage and channel characteristics of millimeter wave band using ray tracing," in *Proc. IEEE Int. Conf. Commun. (ICC)*, London, U.K., Jun. 2015, pp. 1380–1385.
- [30] S. Rajagopal, S. Abu-Surra, Z. Pi, and F. Khan, "Antenna array design for multi-Gbps mmWave mobile broadband communication," in *Proc. IEEE Global Telecommun. Conf. (GLOBECOM)*, Kathmandu, Nepal, Dec. 2011, pp. 1–6.



NASER AL-FALAHY received the B.Sc. and M.Sc. degrees in electronic and communications from Al-Nahrain University, Baghdad, Iraq, in 2001 and 2005, respectively. He is currently pursuing the Ph.D. degree in wireless telecommunication with the University of Salford, Manchester, U.K.

From 2005 to 2010, he was with Motorola for mobile networks provision and network optimization. His research interests include mobile communications, radio network planning and optimization, and millimeter wave communications.



OMAR Y. K. ALANI received the degree in electrical engineering and the M.B.A. degree from the Salford Business School, in addition to other professional certificates in the field of computer networks, and the Ph.D. degree in telecommunication engineering from De Montfort University, U.K., in 2005. He was a Lecturer of telecommunication systems with De Montfort University until 2006, and then a Researcher with the Institute of Advanced Telecommunication, Swansea University. In 2007, he joined the School of Electrical and Electronic Engineering, University of Leeds, as a Research Fellow until 2009. He is currently the Program Leader of computer networks with the School of Computing, Science and Engineering, University of Salford, U.K. He has authored over 60 papers in high-quality journals and conferences proceedings in the field of telecommunications and networking. His research interests include 5G systems, wireless multimedia communications, radio resource management and location/mobility management in next-generation mobile communication systems, diversity and adaptive modulation techniques, and ad hoc and sensors networks.

...